

3. Dvoretzky, A. & Erdős, P. in *Proc. 2nd Berkeley Symp.* 33 (University of California, Berkeley, 1951).
4. Vineyard, G. H. *J. math. Phys.* **4**, 1191–1193 (1963).
5. Beeler, R. J. & Delaney, J. A. *Phys. Rev.* **A130**, 962–966 (1963).
6. Beeler, R. J. *Phys. Rev.* **A134**, 1396–1401 (1964).
7. Rosenstock, H. B. *Phys. Rev.* **A187**, 1166–1168 (1969).
8. Montroll, E. W. in *Stochastic Processes in Applied Mathematics* XVI, 193–220 (American Mathematical Society, Providence, 1964).
9. Montroll, E. W. & Weiss, G. H. *J. math. Phys.* **6**, 167–177 (1965).
10. Jain, N. C. & Orey, S. *Israel J. Math.* **6**, 373–380 (1968).
11. Henyey, F. S. & Seshadri, V. *J. chem. Phys.* **76**, 5530–5534 (1982).
12. Torney, D. C. *J. stat. Phys.* **44**, 49–66 (1986).
13. Skellam, J. G. *Biometrika* **38**, 196–218 (1951).
14. Skellam, J. G. *Biometrika* **39**, 346–362 (1952).
15. Pielou, E. C. *An Introduction to Mathematical Ecology* (Wiley-Interscience, New York, 1969).
16. Edelman-Keshet, L. *Mathematical Models in Biology* (Random House, New York, 1988).
17. Smoluchowski, M. v. *Z. phys. Chem.* **29**, 129 (1917).
18. Rice, S. A. *Diffusion-Controlled Reactions* (Elsevier, Amsterdam, 1985).
19. Haus, J. W. & Kehr, K. W. *Physics Rep.* **150**, 263–416 (1987).
20. Havlin, S. & Ben-Avraham, D. *Adv. Phys.* **36**, 695–798 (1987).
21. Bouchaud, J.-P. & Georges, A. *Physics Rep.* **195**, 127–293 (1990).
22. Bunde, A. & Havlin, S. (eds) *Fractals and Disordered Systems* (Springer, Berlin, 1991).
23. Barber, M. N. & Ninham, B. W. *Random and Restricted Walks* (Gordon & Breach, New York, 1970).
24. Berg, H. C. *Random Walks in Biology* (Princeton University Press, 1983).
25. Weiss, G. H. & Rubin, R. J. *Adv. chem. Phys.* **52**, 363–475 (1983).

ACKNOWLEDGEMENTS. We thank M. Araujo, A. L. Barabasi, G. Huber, J. Lee and P. H. Poole for discussions, and CONACYT, ONR, NSF and the US–Israel Binational Foundation for support.

Crumpled and collapsed conformations in graphite oxide membranes

Xin Wen*, Carl W. Garland*, Terence Hwa†, Mehran Kardar*, Etsuo Kokufuta‡, Yong Li*, Michal Orkisz* & Toyochi Tanaka*

* Center for Materials Science and Engineering, Massachusetts Institute of Technology, Cambridge, Massachusetts 02139, USA

† Physics Department Harvard University, Cambridge, Massachusetts 02138, USA

‡ Institute of Applied Biochemistry, University of Tsukuba, Tsukuba, Ibaraki 305, Japan

MEMBRANES composed of bilayers of amphiphiles such as phospholipids generally exhibit two-dimensional liquid-like structure within the layers. When the constituent molecules of such a membrane are permanently cross-linked to each other, the membrane becomes less flexible, forming a two-dimensional solid. Solid membranes are expected to exhibit very different behaviour from their liquid counterparts^{1–3}, including transitions between a two-dimensional flat phase, a crumpled phase of fractal dimension 2.5 and a compact, three-dimensional phase. Experimental evidence for the crumpled phase has, however, been lacking. As this phase was not observed in computer simulations^{4–6}, it has been suggested that it may always be absent for self-avoiding (and therefore all real) membranes^{4–6}. To the contrary, we report here the experimental observation of the crumpled conformation in an aqueous suspension of graphite oxide membranes. Static light scattering measurements indicate the presence of membrane conformations with a fractal dimension of 2.54 ± 0.05 . As the intra-membrane affinity is enhanced by changing the composition of the solvent, the membranes collapse to a compact configuration.

A natural state for a solid membrane is a flat configuration. Unlike in a liquid membrane which lacks internal shear elasticity, out-of-plane thermal undulations in a solid membrane are not energetically favoured, because they are accompanied by in-plane strains⁷. When the in-plane elasticity is sufficiently weak or the temperature high enough, it has been argued that a crumpled conformation with random orientations should form because the entropy gain from the increased number of bent and folded configurations more than compensates the internal energy cost^{7,8}. Like the coiled polymer, the crumpled membrane is a tenuous fractal⁹ with a dimension determined by the competition between the configurational entropy and steric constraints. If the affinity between the molecules is increased, the membrane

may collapse completely into a compact configuration^{10,11}. Figure 1 provides a schematic representation of these three phases.

In computer simulations^{4–6}, flat and compact^{10,11} conformations have been realized by tuning simple potentials, but the intermediate crumpled phase has not been observed in equilibrium. This has led to the conjecture that a crumpled phase is always absent in self-avoiding membranes⁷. Experimental studies of solid membranes are therefore most desirable. Candidates for solid membranes include sheets of graphite oxide (GO)^{12–15} and MoS₂ (ref. 16), the spectrin network extracted from red blood cells (C. Schmitt, personal communication) and polymerized liquid membranes¹⁷. Previous electron microscope images show that both GO¹⁵ and MoS₂ (ref. 16) form irregular and folded configurations when dried on the microscope stage. Here we study conformations of GO membranes suspended in dilute solution.

GO membranes are synthesized by exfoliating bulk graphite with strong oxidizing agents^{12,13,15}; we used potassium permanganate. The product of the oxidation reaction is GO, brownish yellow in colour, which consists of carbon layers bonded by oxygens¹⁴. Electron microscopy has shown that the GO membranes have a crystalline internal order¹⁵ and can be as thin as one carbon layer¹⁴. Hydroxyl (OH) groups are bound to the surfaces of the GO membranes¹⁴. These hydroxyl groups, capable of forming hydrogen bonds with water molecules, are responsible for the compatibility of GO with aqueous solutions.

A light scattering study of the structure of membranes in solution requires some control over their sizes. This was achieved by using polycarbonate filters (Nucleopore). The GO suspension was sequentially passed through filters with 8- μ m and 3- μ m pore size. The membranes retained on the 3- μ m filter were redispersed in a solution, with the original buffer conditions. The final solution contains GO membranes sized between 3 and 8 μ m with a concentration of ~ 0.01 wt%.

In static laser-scattering experiments, conformations of GO membranes are probed through the structure factor, $S(q)$, at a wave vector q , which is directly related to the radius of gyration, R_G , and to the fractal dimension⁹, d_f , of the scattering objects. The membrane conformations can be differentiated by their fractal dimensions: for a flat membrane, $d_f = 2$, whereas a compact conformation corresponds to $d_f = 3$. The fractal dimension of the intermediate crumpled phase is estimated to be 2.5, from a Flory argument³. For a monodisperse solution^{3,18}, $S(q) \approx 1 - (qR_G)^2/2$ for $qR_G < 1$, and $S(q) \approx q^{-d_f}$ for $qR_G > 1$. As our solutions are polydisperse, the power law should be checked only at length scales shorter than the size of the smallest GO membranes (3 μ m). As our shortest probing length is 0.2 μ m (half of the laser wavelength), we have a range of about 1.5 decades in q to determine the scaling exponent d_f for the decay of $S(q)$.

Figure 2 illustrates the structure factors of GO membranes obtained from aqueous solutions at three pH values. The behaviour of $S(q)$ is fairly consistent with a self-similar scaling of density fluctuations at length scales less than the size of membranes. The best fits give a value of $d_f = 2.54 \pm 0.05$, very close to the theoretical estimate³ of 2.5. The fractal dimension was found to be insensitive to pH and salt concentrations. This is understandable considering the low density of the ionizable groups (one COOH group for every fifty carbons¹⁴). When 10% acetone is added to the solution, the structure factor, shown in Fig. 3, suggests formation of a compact conformation with a fractal dimension of ~ 3 , and a somewhat smaller radius of gyration. This observation can be explained by the fact that acetone molecules are less polar than water molecules. On addition of acetone, the solvent becomes poorer, and the intra-membrane affinity is enhanced.

Although our observation of a fractal dimension of ~ 2.5 is consistent with a crumpled phase of membranes, we also consider some other possible explanations. Haphazard crushing of

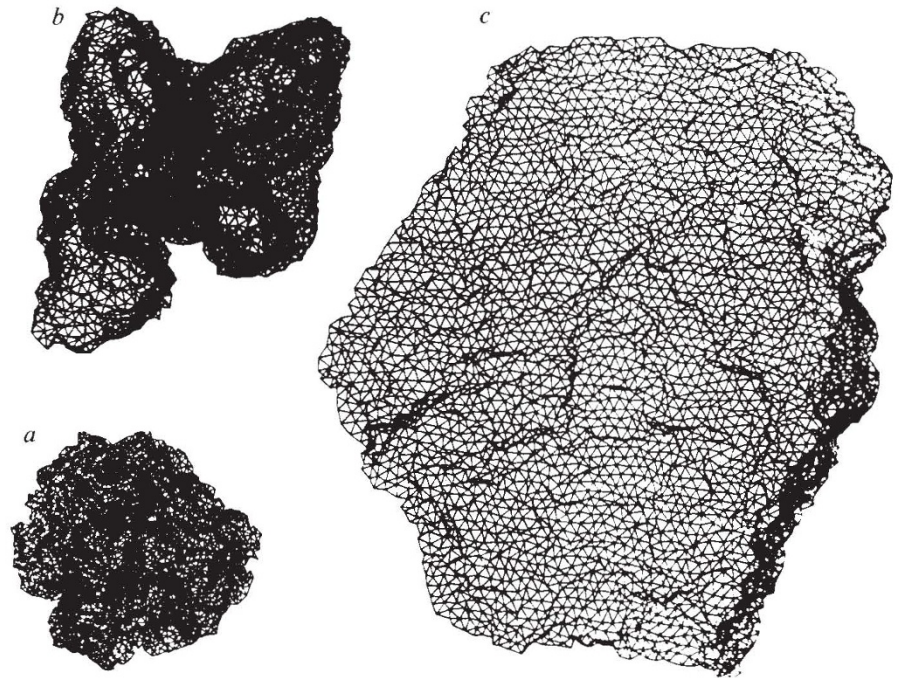


FIG. 1 Schematic representations of (a) compact, (b) crumpled and (c) flat conformations of solid membranes. These illustrations, taken from ref. 11, actually correspond to the same membrane at three different times in a numerical relaxation. This sequence also illustrates the need to complement static light-scattering results with dynamical studies.

foil or paper^{19,20} also leads to objects with a fractal dimension of ~ 2.5 . Such objects are, however, far from equilibrium and represent metastable states along the way to a fully compact conformation. The observation of a separate collapsed phase is evidence against this. Another possibility is a mixture of flat and compact configurations. This is unlikely in view of the lack of any curvature in the data of Fig. 2. On a log-log scale, light scattering data from a mixture of fractals of dimensions 2 and 3 would show clear bending in an interval of two decades

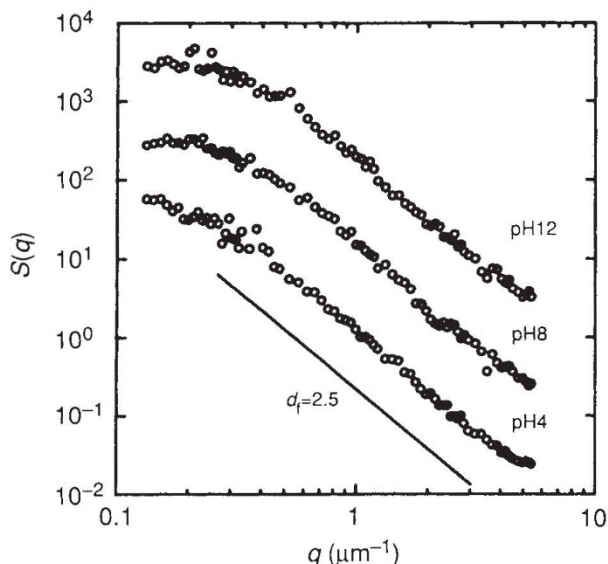


FIG. 2 The structure factor, $S(q)$, of GO membranes (sizes 3 to 8 μm) in aqueous solution at different pH. All measurements were made at room temperature. The wavevector is defined as $q=1/\lambda$, where λ is the wavelength of the density wave that scatters the incident laser beam. The data for pH 8 and pH 12 have been shifted vertically for clarity. For $q > 0.33 \mu\text{m}^{-1}$, the plots of $\log S(q)$ against $\log q$ can be fitted to straight lines, indicating that the GO membranes are self-similar at length scales smaller than their sizes. The fractal dimensions given by the fittings are: 2.55 ± 0.02 for pH 4, 2.56 ± 0.03 for pH 8, and 2.51 ± 0.03 for pH 12. The theoretical estimate of a fractal dimension of 2.5 for a crumpled conformation is indicated for comparison by the solid line.

(D. A. Weitz, personal communication). Finally, flat membranes whose thickness scales with lateral size are inconsistent with our observations, as they would also produce a large curvature in $\log q$ - $\log S(q)$ plots¹⁵.

Our experimental results therefore indicate that a crumpled conformation exists in solid membranes. This is somewhat surprising, as most numerical simulations of rather flexible self-avoiding membranes produce flat conformations⁴⁻⁶. The flat phase is, however, unstable to a glassy crumpled configuration in the presence of internal defects²¹. More information on the microstructure of GO, its rigidity and characteristic defects is needed. To determine the nature of the crumpled state, we propose three experimental studies. First, X-ray scattering experiments should be performed to reveal the mean curvatures and defects in GO membranes at microscopic scales. Second, the crumpled-to-compact transition should be systematically

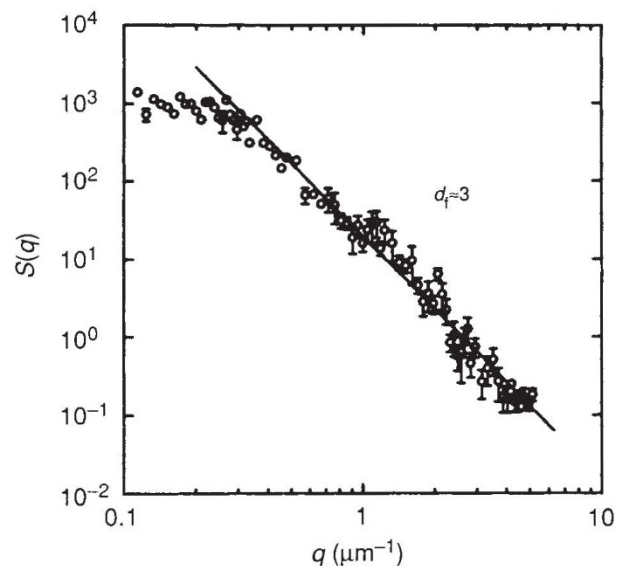


FIG. 3 The structure factor, $S(q)$, of GO membranes in a 10% acetone + water solution with pH 4. The slope at $q > 0.33 \mu\text{m}^{-1}$ is ~ 3 (3.10 ± 0.05), and the radius of gyration is somewhat smaller than in aqueous solutions, indicating a compact conformation of GO membranes.

studied with varying acetone concentrations and/or varying temperature at a suitable acetone concentration. A careful study of the reversibility of this transition could definitely test the existence of these two phases as distinct stable states. Third, a careful dynamic light-scattering study could reveal the relaxation times of the internal modes of the membranes, and thus distinguish between equilibrium and possible glassy conformations^{19–21}. Preliminary dynamic light-scattering data show two dynamic modes, the slower of which has a relaxation time roughly proportional to q^{-2} and may correspond to brownian diffusion of the GO membranes. Further studies are in progress. □

Received 28 May; accepted 24 October 1991.

- Lipowsky, R. *Nature* **349**, 475–481 (1991).
- Statistical Mechanics of Membranes and Surfaces* (eds Nelson, D. R., Piran, T. & Weinberg, S.) (World Scientific, Singapore, 1989).
- Kantor, Y., Kardar, M. & Nelson, D. R. *Phys. Rev. Lett.* **57**, 791–794 (1986); *Phys. Rev. A* **35**, 3056–3071 (1987).
- Plischke, M. & Boal, D. H. *Phys. Rev. A* **38**, 4943–4945 (1988).
- Abraham, F. F., Rudge, W. E. & Plischke, M. *Phys. Rev. Lett.* **62**, 1757–1759 (1989).
- Ho, J.-S. & Baumgartner, A. *Phys. Rev. Lett.* **63**, 1324 (1989).
- Kantor, Y. & Nelson, D. R. *Phys. Rev. Lett.* **58**, 2774–2777 (1987).
- Paczuski, M., Kardar, M. & Nelson, D. R. *Phys. Rev. Lett.* **60**, 2638–2640 (1988).
- Mandelbrot, B. *The Fractal Geometry of Nature* (Freeman, San Francisco, 1982).
- Abraham, F. F. & Kardar, M. *Science* **252**, 419–422 (1991).
- Abraham, F. F. & Nelson, D. R. *J. Phys. (France)* **51**, 2653–2672 (1990).
- Brodie, B. *Phil. Trans.* **149**, 249–251 (1859).
- Hummers, W. S. & Offeman, R. E. *J. Am. chem. Soc.* **80**, 1339 (1958).
- Boehm, H. P., Glauss, A., Fischer, G. & Hofmann, U. *Z. Naturforsch.* **17**, 150–153 (1962).
- Hwa, T., Kokufuta, E. & Tanaka, T. *Phys. Rev. A* **44**, R2235–R2237 (1991).
- Chianelli, R. R., Prestridge, E. B., Pecoraro, T. A. & DeNeufville, J. P. *Science* **203**, 1105–1107 (1979).
- Mutz, M., Bensimon, D. & Brienne, M. J. *Phys. Rev. Lett.* **67**, 923–926 (1991).
- Martin, J. E. & Hurd, A. J. *J. appl. Cryst.* **20**, 61–78 (1987).
- Gomes, M. A. F., & Vasconcelos, G. L. *Phys. Rev. Lett.* **60**, 237 (1988).
- Kantor, Y., Kardar, M. & Nelson, D. R. *Phys. Rev. Lett.* **60**, 238 (1988).
- Nelson, D. R. & Radzihovsky, L. *Europhys. Lett.* **16**, 79–84 (1991).

ACKNOWLEDGEMENTS. We thank D. R. Nelson, D. A. Weitz, T. A. Witten and Y. Q. Zhang for discussions. This research is supported by NSF grants to the CMSE at MIT.

Magic numbers and stable structures for fullerenes, fullerides and fullerenium ions

Patrick W. Fowler* & David E. Manolopoulos†

* Department of Chemistry, University of Exeter, Exeter EX4 4QD, UK

† Department of Chemistry, University of Nottingham, Nottingham NG7 2RD, UK

MACROSCOPIC amounts of the two fullerenes C_{60} and C_{70} have been available for a year¹, and have already had an enormous impact on research in chemistry and physics. Experimentalists are now turning their attention to the higher fullerenes^{2,3}. Qualitative molecular-orbital theory predicts^{4–6} stability for C_n with $n = 60, 70, (72), 76, 78, 84, \dots$, of which all but C_{72} have now been produced by evaporation of graphite^{1–3}, and in general for infinite series of closed-shell neutral fullerenes for $n = 60 + 6k$ ($k \neq 1$), $70 + 30k$, $84 + 36k$ (all k)^{7–9}. Recent experimental observations of endohedral LaC_n metallofullerenes¹⁰ have been rationalized in terms of 'magic numbers' for fulleride anions C_n^{2-} , for which special stability is predicted¹¹ at $n = 74, 82, 88, \dots$; but the exact extent of charge transfer in these complexes has yet to be determined. Here we present calculations of magic numbers in the fullerenium sequence C_n^{2+} ($n = 74, 80, (88), 92$) and show that the electron count determines stability and the atom count determines structure in all three (neutral, anionic and cationic) series. Stable cations have two carbons more, and stable anions two carbons less, than the corresponding stable neutral cluster. We predict likely structures of the 'magic' cations.

Qualitative theoretical treatments of carbon cages are based on the fullerene hypothesis: that stable structures are pseudo-spherical polyhedra with $(n/2 + 2)$ faces, of which 12 are pen-

tagonal and the remainder hexagonal. The pentagons are needed for geometric closure, and the hexagons maximize the π -delocalization energy of these unsaturated molecules. Within the fullerene constraint, many isomeric forms of C_n are in principle possible, but stable structures have the following features in common: (1) isolated (non-adjointing) pentagons; (2) large π -bonding delocalization energies and large gaps between occupied and empty orbitals; and (3) low steric strain. The pentagon-isolation criterion has been elevated to the status of a rule (the IPR)¹²; it can be rationalized on steric grounds as a way of easing σ -strain¹³, and on electronic grounds as a way of avoiding the anti-aromatic eight-atom cycles inherent in pairs of adjacent pentagons⁴. Large delocalization energies and large gaps between the highest occupied and lowest unoccupied molecular orbitals are obviously conducive to electronic stability, and geometric (geodesic) stability of the cage framework is covered by criterion (3).

When n belongs to one of the special series $60 + 6k$, $70 + 30k$ or $84 + 36k$, candidate structures can be generated by the geometric leapfrog and carbon-cylinder constructions of refs 7–9. These constructions, of which one works by capping all faces and then taking the dual of a smaller fullerene, and the other by equatorial expansion of five- and six-fold symmetric fullerenes, automatically yield isolated-pentagon structures, and so satisfy the IPR. More generally, a computer search for all possible fullerene isomers of any given C_n cage can be carried out with the aid of the ring-spiral algorithm of ref. 14. This algorithm 'peels' each cage as a continuous spiral strip of edge-sharing pentagons and hexagons. The placing of the 12 pentagons in the sequence uniquely determines the adjacency matrix and hence the three-dimensional isomeric form of the fullerene. The three-dimensional structures are thus encoded in a compact one-dimensional representation. Structures with fused pentagons are easily detected and eliminated as the search proceeds. The general isomer count rises rapidly with n (from only 1 for $n = 20$ to over 20,000 for $n = 78$, for example⁵). The count of structures with isolated pentagons also increases rapidly (from only 1 for $n = 60$ to over 450 for $n = 100$), but is much smaller for the same value of n .

Relative stabilities of isolated-pentagon structures for neutral fullerenes depend on a balance between the electronic and steric criteria mentioned above. The leapfrog and carbon cylinder series give all the fullerenes with formally closed-shell electronic structure, but other isomers may still have considerable electronic stability, albeit with slightly bonding LUMOs in simple Hückel theory. The electronic-steric balance is clearly a delicate one. Thus C_{76} is found^{3,4} to be D_2 (electronically favoured over the only other (T_d) isolated-pentagon isomer), whereas^{5,15} the predominant isomer of C_{78} is C_{2v} (sterically favoured over the four other isolated-pentagon isomers, one of which has a closed shell). Prediction of stability from molecular-orbital models or molecular mechanics¹⁵ may therefore be a delicate matter. Nevertheless, steric strain effects being equal, leapfrog and

TABLE 1 Maximum energy gaps Δ^{2+} for isolated-pentagon isomers of fullerenium cations C_n^{2+}

n	Δ^{2+}	n	Δ^{2+}
70	0.0887	84	0.2259
72	0	86	0.2417
74	0.3371*	88	0.3121
76	0.1989	90	0.2138
78	0.2426	92	0.3147*
80	0.4195*	94	0.2906
82	0.2368		

* Local maximum in Δ^{2+} corresponding to a single isomer that also has the highest π -bonding delocalization energy for the given value of n . Energies Δ^{2+} are in units of a single effective Hückel resonance integral β .